



**HAL**  
open science

## ARF1-related disorder: phenotypic and molecular spectrum

Jean-Madeleine de Sainte Agathe, Ben Pode-Shakked, Sophie Naudion, Vincent Michaud, Benoit Arveiler, Patricia Fergelot, Jean Delmas, Boris Keren, Céline Poirsier, Fowzan S Alkuraya, et al.

► **To cite this version:**

Jean-Madeleine de Sainte Agathe, Ben Pode-Shakked, Sophie Naudion, Vincent Michaud, Benoit Arveiler, et al.. ARF1-related disorder: phenotypic and molecular spectrum. *Journal of Medical Genetics*, 2023, 10.1136/jmg-2022-108803 . hal-04191246

**HAL Id: hal-04191246**

**<https://hal.sorbonne-universite.fr/hal-04191246>**

Submitted on 30 Aug 2023

**HAL** is a multi-disciplinary open access archive for the deposit and dissemination of scientific research documents, whether they are published or not. The documents may come from teaching and research institutions in France or abroad, or from public or private research centers.

L'archive ouverte pluridisciplinaire **HAL**, est destinée au dépôt et à la diffusion de documents scientifiques de niveau recherche, publiés ou non, émanant des établissements d'enseignement et de recherche français ou étrangers, des laboratoires publics ou privés.



Distributed under a Creative Commons Attribution - NonCommercial 4.0 International License



Original research

# ARF1-related disorder: phenotypic and molecular spectrum

Jean-Madeleine de Sainte Agathe <sup>1</sup>, Ben Pode-Shakked <sup>2,3</sup>, Sophie Naudion,<sup>4</sup> Vincent Michaud <sup>4,5</sup>, Benoit Arveiler,<sup>4,5</sup> Patricia Fergelot,<sup>4,5</sup> Jean Delmas <sup>6</sup>, Boris Keren,<sup>1</sup> Céline Poirsier,<sup>7</sup> Fowzan S Alkuraya <sup>8</sup>, Brahim Tabarki,<sup>9</sup> Eric Bend <sup>10</sup>, Kellie Davis,<sup>11</sup> Martina Bebin <sup>12</sup>, Michelle L Thompson <sup>13</sup>, Emily M Bryant <sup>14</sup>, Matias Wagner <sup>15,16</sup>, Iris Hannibal,<sup>17</sup> Jerica Lenberg,<sup>18</sup> Martin Krenn <sup>19</sup>, Kristen M Wigby,<sup>20</sup> Jennifer R Friedman,<sup>21,22</sup> Maria Iascone <sup>23</sup>, Anna Cereda <sup>24</sup>, Térence Miao,<sup>1,25</sup> Eric LeGuern <sup>1,26</sup>, Emanuela Argilli,<sup>27</sup> Elliott Sherr,<sup>27</sup> Oana Caluseriu,<sup>28</sup> Timothy Tidwell,<sup>29</sup> Pinar Bayrak-Toydemir,<sup>30</sup> Caroline Hagedorn,<sup>31</sup> Melanie Brugger <sup>32</sup>, Katharina Vill,<sup>33</sup> Francois-Dominique Morneau-Jacob,<sup>34</sup> Wendy Chung <sup>35</sup>, Kathryn N Weaver <sup>2</sup>, Joshua W Owens,<sup>2</sup> Ammar Husami <sup>2</sup>, Bimal P Chaudhari,<sup>36,37,38</sup> Brandon S Stone,<sup>39</sup> Katie Burns,<sup>40</sup> Rachel Li,<sup>41</sup> Iris M de Lange,<sup>42</sup> Margaux Biehler,<sup>43</sup> Emmanuelle Ginglinger,<sup>44</sup> Bénédicte Gérard,<sup>43</sup> Rolf W Stottmann,<sup>2,45</sup> Aurélien Trimouille <sup>4,5,46</sup>

► Additional supplemental material is published online only. To view, please visit the journal online (<http://dx.doi.org/10.1136/jmg-2022-108803>).

For numbered affiliations see end of article.

## Correspondence to

Dr Jean-Madeleine de Sainte Agathe, Department of Medical Genetics, Sorbonne University Faculty of Medicine, Paris, 75013, France; jean-madeleine.desainteagathe@aphp.fr

Received 9 August 2022  
Accepted 7 April 2023



© Author(s) (or their employer(s)) 2023. Re-use permitted under CC BY-NC. No commercial re-use. See rights and permissions. Published by BMJ.

## To cite:

de Sainte Agathe J-M, Pode-Shakked B, Naudion S, et al. *J Med Genet* Epub ahead of print: [please include Day Month Year]. doi:10.1136/jmg-2022-108803

## ABSTRACT

**Purpose** *ARF1* was previously implicated in periventricular nodular heterotopia (PVNH) in only five individuals and systematic clinical characterisation was not available. The aim of this study is to provide a comprehensive description of the phenotypic and genotypic spectrum of *ARF1*-related neurodevelopmental disorder.

**Methods** We collected detailed phenotypes of an international cohort of individuals (n=17) with *ARF1* variants assembled through the GeneMatcher platform. Missense variants were structurally modelled, and the impact of several were functionally validated.

**Results** De novo variants (10 missense, 1 frameshift, 1 splice altering resulting in 9 residues insertion) in *ARF1* were identified among 17 unrelated individuals. Detailed phenotypes included intellectual disability (ID), microcephaly, seizures and PVNH. No specific facial characteristics were consistent across all cases, however microretrognathia was common. Various hearing and visual defects were recurrent, and interestingly, some inflammatory features were reported. MRI of the brain frequently showed abnormalities consistent with a neuronal migration disorder.

**Conclusion** We confirm the role of *ARF1* in an autosomal dominant syndrome with a phenotypic spectrum including severe ID, microcephaly, seizures and PVNH due to impaired neuronal migration.

## INTRODUCTION

Periventricular nodular heterotopia (PVNH) is a neuronal migration disorder consisting of ectopic neuronal nodules along the lateral ventricles.

## WHAT IS ALREADY KNOWN ON THIS TOPIC

⇒ *ARF1*-related disorder has been previously described as a syndromic intellectual disability associated with periventricular nodular heterotopia, but with a limited number of cases, most of them are poorly phenotyped.

## WHAT THIS STUDY ADDS

⇒ This study reports the first detailed phenotyped cohort of 17 individuals with variants in *ARF1*.

## HOW THIS STUDY MIGHT AFFECT RESEARCH, PRACTICE OR POLICY

⇒ This study implicates *ARF1* in a more nuanced phenotype, suggesting a possible relevance for growth parameters or inflammatory manifestations surveillance.

⇒ This study also recommends the specific use of Mistic predictor (>0.9) to discriminate between pathogenic and benign missense variants.

Seizures, microcephaly and intellectual disability (ID) are frequently associated with PVNH.<sup>1</sup>

Neuronal migration during human cortical development is dependent on a wide range of interconnected cellular processes such as actin and microtubule cytoskeleton regulation, cell-cell adhesion, apical adhesion, junction formation, vesicle trafficking and membrane protein turnover. Disruption of these processes can lead to periventricular heterotopia where neurons are unable to properly migrate into the developing cortical plate.<sup>1,2</sup>

## Developmental defects

ADP-ribosylation factor proteins (ARF1/3/4/6) are anchored to the membrane via N-terminal myristoylation.<sup>3</sup> At the membrane, ARF1 acts as a molecular switch thanks to a transition between two structural conformations: inactive when bound to guanosine diphosphate (GDP), and active when bound to guanosine triphosphate (GTP). ARF1 activation is induced by Guanine Exchange Factors, such as ARFGEF2, which remove the GDP, triggering the GDP to GTP exchange. This causes a conformational change allowing ARF1 to bind different targets, notably through a shift of the loop from Leu39 to Ile49. ARF1<sup>GTP</sup> promotes trans-Golgi network through the recruitment of clathrin adaptor proteins and the fission step of the vesicle formation. As the vesicle is budding, ARF1 dimerisation is required to continue the coat-omer polymerisation, notably when the slimming neck of the bud prohibits ARF1's further anchorage to the lipid bilayer.<sup>4</sup> ARF1-dependent endocytosis has been strongly implicated in PVNH because of its association with genetic alterations of *FLNA* (MIM: 300049), *ARFGEF2* (MIM: 608097) and *ARF1* (MIM: 618185) but clinical evidence to date is based on only five cases.<sup>5–7</sup>

The aim of this study is to further describe the phenotypic spectrum of *ARF1*-related disorder as we report a robust cohort of 17 individuals harbouring de novo pathogenic or likely pathogenic variants in *ARF1*.

## MATERIALS AND METHODS

Previously unreported individuals harbouring de novo *ARF1* variants were recruited using GeneMatcher.<sup>8</sup> In addition, two previously reported individuals have been included: the detailed unpublished clinical and radiographic information were collected on an individual previously included in a large cohort of >2200 families with various Mendelian phenotypes and the updated phenotype of one previously published individual has been obtained.<sup>6</sup>

Phenotypic and genotypic information was obtained using a standardised questionnaire to evaluate clinical, electroencephalography (EEG) and brain MRI (bMRI) findings as well as genetic variant information. Variants were identified using trio exome sequencing (ES) or genome sequencing (GS) as trio, duo

or singleton analyses (table 1). When photos were available, a specific informed consent was obtained from the parents. When available, the bMRI findings were re-evaluated by a single neuroradiologist.

Variants were interpreted using the American College of Medical Genetics and Genomics/Association for Molecular Pathology guidelines.<sup>9</sup> The effects of missense variants were predicted by several in silico tools (table 1, online supplemental figure 1), and mapped to the missense tolerance landscape from MetaDome.<sup>10</sup>

The pathogenicity of five missense variants was further supported by in vitro functional pulldown assays. We functionally analysed ARF1 activation for four of the patient variants (p.Thr48Ile, p.Phe51Leu, p.Arg99His, p.Lys127Glu) as previously reported for p.Y35H.<sup>5</sup> For reproducibility, p.Y35H was also included. Each of the five variants was introduced by site-directed mutagenesis into the *ARF1* myc-tagged cDNA (plasmid pCMV6-ARF1-myc, transcript NM\_001130408, GenScript, Piscataway, New Jersey, USA), and verified by sequencing prior to transfection (DNA Sequencing and Genotyping Core, CCHMC). Plasmids with reference and mutant sequences were transfected into HEK293T cells in 10 cm<sup>2</sup> plates, using the Lipofectamine 3000 Transfection Kit (Invitrogen, Thermo Fisher, Waltham, Massachusetts, USA). HEK293T cells were cultured in Dulbecco's Modified Eagle's Medium with 10% fetal bovine serum, 2 mM L-glutamine, Penicillin-Streptomycin per manufacturer's recommendations. To assess activated ARF1, GST-GGA3 pulldown was performed on cell lysates prior to western blot analysis, using the Active ARF1 Pull-Down and Detection Kit (Thermo Fisher, Waltham, Massachusetts, USA), per manufacturer's instructions. Processing of samples was performed at 4°C and followed by incubation with GST-GGA3-PBD for 1 hour. For western immunoblotting, anti-ARF1 rabbit monoclonal IgG as primary antibody was diluted at 1:2000 in Intercept buffer prior to incubation at –4°C for 24 hours under agitation. The blot was then incubated with IRDye 800CW Goat antirabbit antibody at 1:15 000 dilution for 1 hour at room temperature under agitation. Western blot analysis results were imaged using Odyssey Sa IFred scanner (LI-COR, Bad Homburg, Germany), equipped with Imaging Studio (Analysis Software V.4.0). Results were quantified using Empiria Studio V.1.3 software. The experiment was performed three times.

Whole blood was collected on PAXgen tube and total RNA was extracted from patient's lymphoblastoid cell lines using PAXgene Blood RNA kit (Qiagen). cDNA was generated from 1 µg RNA with the addition of random hexamers and oligo dT primers using the SuperScript II Reverse Transcriptase (ThermoFisher Scientific). Impact on transcription of the c.384+1G>T substitution was then characterised by PCR Sanger sequencing on cDNA according to standard procedures, using primers localised in exons 3 and 5 of *ARF1* gene, (F=ACCGTGGAGTACAAGA ACATCAGC, R=ACTTCTGGTTCGGAGCTGAT).

Structural consequence of missense variants were predicted using SwissModel<sup>11</sup> (V.4.1.0), DynaMut2<sup>12</sup> and visualised with Mol\*.<sup>13</sup>

## RESULTS

### Clinical findings

The 17 individuals (9 females, 8 males) heterozygous for de novo *ARF1* variants ranged in age from 16 months to 14 years (online supplemental table 1). The recurrent substitution c.296G>A; p.(Arg99His) was found in four unrelated individuals, resulting in a total of five different de novo occurrences, including the

**Table 1** Clinical characteristics of the cohort

	Prevalence	This study	Ge <i>et al</i> <sup>5</sup>	Gana <i>et al</i> <sup>7</sup>
Intellectual disability	100%	14/14	3/3	1/1
Age at walking	27 months	14	0/0	0/0
Speech delay	100%	17/17	2/2	0
First words	19 months	7	0/1	0
Sentences	30%	5/16	0/1	0
ADHD, autism	50%	6/11	1/2	0/1
Microcephaly (<–3 SD)	50%	10/17	0/2	0/1
Head circumference	–1.3 SD	14/17	2/3	1/1
Seizures	48%	8/17	2/3	0/1
Hypotonia	68%	12/17	1/1	0/1
Spasticity	25%	4/17	1/1	0/1
Ataxia	21%	4/17	0/1	0/1
PVNH	30%	4/17	1/3*	1/1
Thin corpus callosum	55%	9/17	1/2	0/1
Growth delay	25%	4/16	1/2	0/1

The three last columns (right) depict the number of informative individuals in each report.

\*The R99H individual in Ge *et al* was incorrectly described with PVNH.

ADHD, attention deficit hyperactivity disorder; PVNH, periventricular nodular heterotopia.

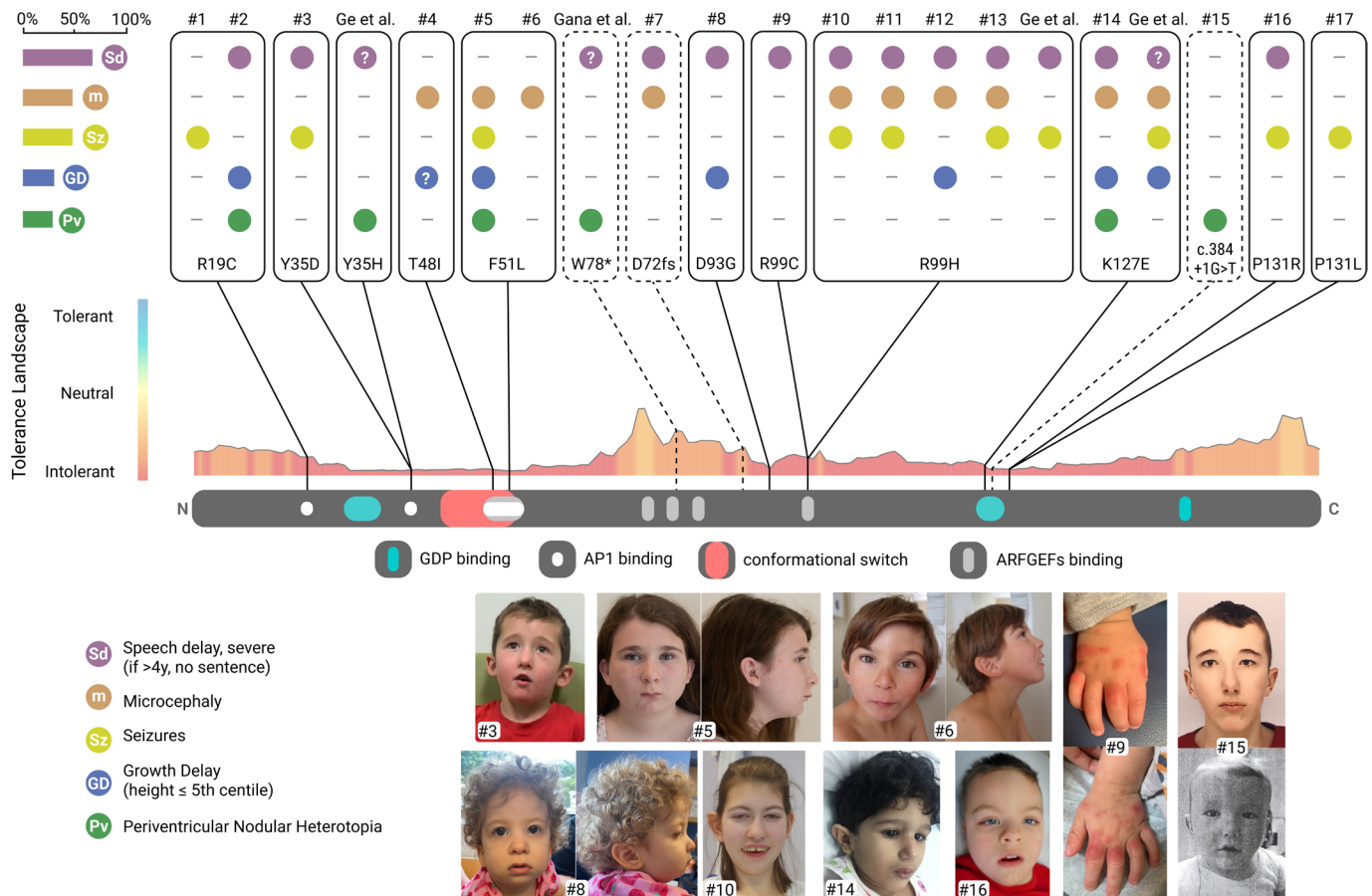


**Figure 1** Clinical overview of 21 individuals with *ARF1* variants (17 individuals from this study, 3 individuals previously reported from Ge *et al*<sup>5</sup> and one from Gana *et al*.<sup>7</sup> Tolerance landscape from MetaDome.<sup>10</sup> Plain lines point to the missense location, dashed lines point to non-missense altered residues (either to the premature terminating codon or to the nine residues insertion).

individual from Ge *et al*<sup>5</sup> (figure 1, for the detailed clinical description of the cohort, see online supplemental table 1).

All individuals with available information presented with varying degrees of ID, ranging from mild to severe. Individuals #2, #7 and #9 (aged 18, 16 and 24 months, respectively) had motor delay along with speech delay, but have not been formally diagnosed with ID.

Microcephaly below 3 SD was noted in 10 individuals (50%; 10/20), seizures of various types were reported in 8 (50%; 8/16) and PVNH in 3 (20%, 3/15). No correlation was found between seizure history and PVNH. bMRI frequently showed abnormalities: small cerebellum (3/20) and neuronal migration defects including PVNH, cortical dysplasia, polymicrogyria (45%; 9/20) and corpus callosum abnormalities (50%; 10/20) (see online supplemental figure 5).

Facial characteristics (figure 1) included micrognathia or retrognathia (26%; 5/19), low-set ears (16%; 3/19), dental malposition (10%; 2/19) and short philtrum (10%; 2/19). Of note, individual #4 had obstructive sleep apnoea secondary to her microretrognathia that benefited from mandibular distraction. Visual or hearing impairments were common (58%; 11/19), and included bilateral profound sensorineural hearing loss, cortical vision impairment, strabismus, astigmatism and hyperopia.

Additional findings included sleep disturbance (32%; 6/19), cardiac defects (16%; 3/19) and hypospadias (2/6 male individuals).

Interestingly, some idiopathic cutaneous or hepatic manifestations were reported, including hand hyperkeratotic skin (individual #3, individuals from Gana *et al*), pernio-like rashes involving the hands, feet, upper helices of the ears (individual #9), idiopathic and persistent elevation of liver enzymes (individuals #8 and #9). For individual #9, a liver biopsy was performed at age 1, showing sparse patchy lobular necroinflammatory lesions, no sign of portal inflammation, no haemochromatosis and negative staining for glycogen storage disease.

### Molecular analysis

Thirteen different de novo variants in *ARF1* (NM\_001658.4; ENST00000272102.10) were identified in 17 individuals: 10 missense variants, 1 splice variant and 1 frameshift variant. (*Nota bene*: the missense p.(Phe51Leu) was caused by two different variants, c.153C>A and c.151T>C.) All variants were absent from gnomAD<sup>14</sup> (V.2.1.1; V.3.1.2) or deCAF<sup>15</sup> and the 10 missense variants were predicted to be deleterious by multiple in silico tools (see ‘Discussion’ section and online supplemental figure 1A). The frameshift variant p.(Asp72Thrfs\*17) is predicted to elicit nonsense-mediated decay according to the 50 nucleotides rule,<sup>16</sup> and is identified by the Loss-Of-Function Transcript Effect Estimator (V.1.0.3<sup>14</sup>) to result in a loss of function with high confidence.

The splice variant c.384+1G>T is predicted by SpliceAI<sup>17</sup> to create an in-frame donor site, resulting in the inclusion of nine residues near the GTP-binding site (online supplemental figure 1B).

No other pathogenic or likely pathogenic variant was reported in any of the cases.

**Structural analysis**

The locations of the 10 missense variants in ARF1 are mostly clustered near the GDP-binding domain (figure 1 and figure 2).

The Arg19 residue is located at a key position of the GDP-GTP switch. In the inactive conformation (GDP-bound), the

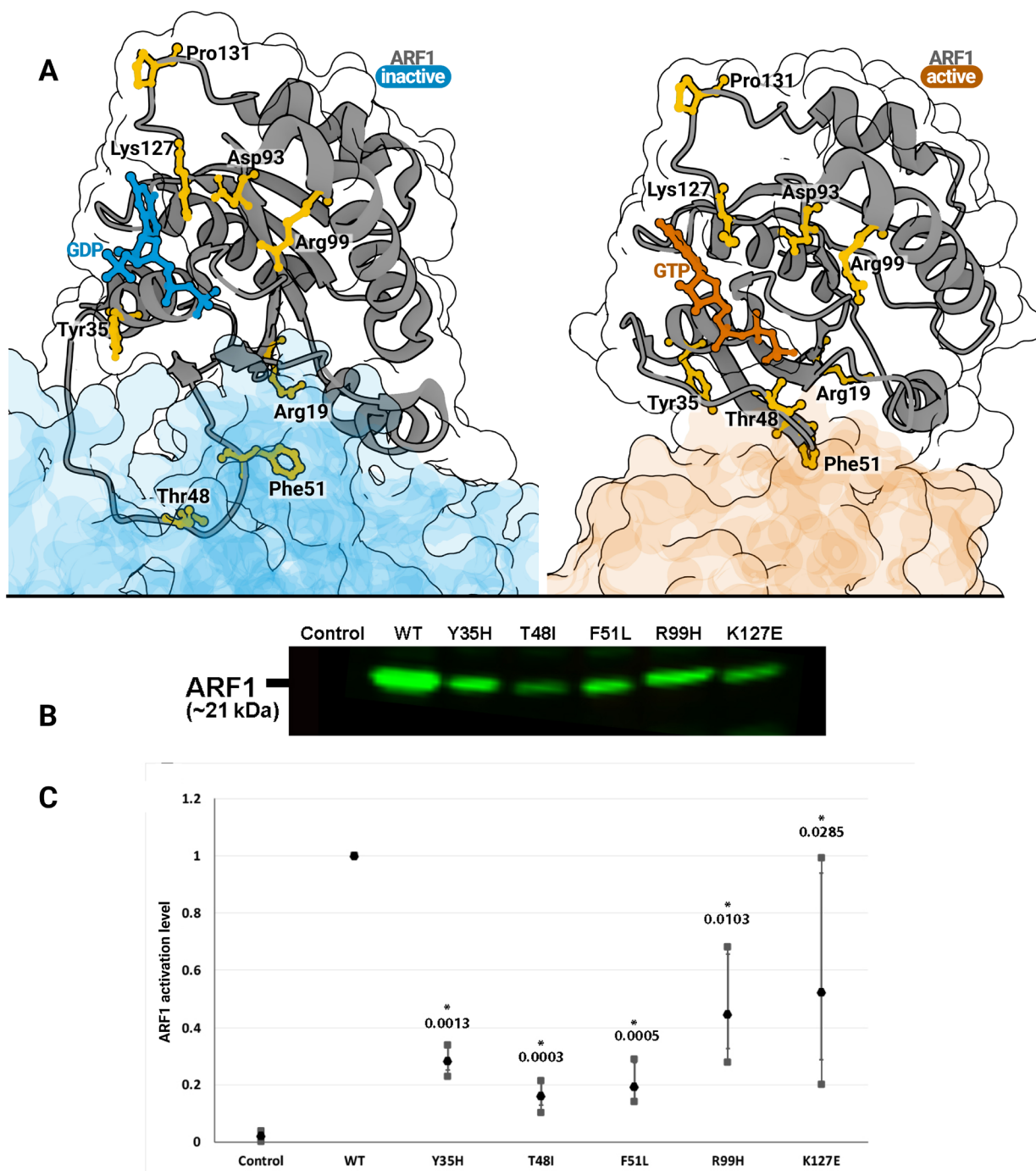


**Figure 2** (A) Locations of the eight residues (yellow) altered in the two conformations of ARF1. Left, ARF1 in its inactive conformation from 1r8q<sup>20</sup>; right, ARF1 in active conformation from 6cm9<sup>36</sup>; blue chain: ARF1; grey chain: ARFGEF sec7 domain. Images created using Mol\*.<sup>13</sup> (B, C) Deleterious effect of patient ARF1 variants on nucleotide activation. Comparison of ARF1 nucleotide activation in lysates of 293 T cells transfected with either the wild-type (WT) ARF1 plasmid or that harbouring one of the five variants (p.Tyr35His, p.Thr48Ile, p.Phe51Leu, p.Arg99His, p.Lys127Glu). Lane 1, basal activated ARF1 in 293 T cells without plasmid transfection. Pulldown for GTP-activated ARF1 in cells transfected with WT (lane 2) vs patient variant-containing ARF1 plasmid (lanes 3–7). ARF1 band is visible at 21 kDa. Western blot analysis results are representative of three independent transfection and pulldown experiments. (C) Quantification of relative nucleotide activation in lysates of 293 T cells transfected with ARF1 plasmids harbouring one of five patient ARF1 variants compared with a WT ARF1 and no plasmid. Mean results are presented as the mean (±SEM) of three separate experiments. P value of the result of each variant in comparison to the WT is presented.

Arg19 sidechain points towards an adjacent helix of ARF1 (via Tyr81), however when ARF1 binds GTP, the sidechain of Arg19 is uncovered by the switch, and binds to ARF1 target (adaptor protein AP-1 complex, gamma-1 subunit, Glu41).

Tyr35 is required for the dimerisation of ARF1 and the Tyr35Ala has been previously shown to prevent in vitro vesicle scission.<sup>4</sup>

Thr48 is directly bound to the third phosphate group of GTP. It has been demonstrated to be crucial for the exchange of GDP for GTP during the activation of ARF1.<sup>18</sup>

Lys127 is part of the conserved NKXD motif, which binds to the guanine ring of GDP (online supplemental figure 2).<sup>19</sup> In ARF1, Lys127 closely interacts with Asp93. Asp93 stabilises the Lys127 sidechain position through a hydrogen bond (online supplemental figure 2).

The Phe51 residue is located in a switching region of ARF1, which penetrates the hydrophobic groove of guanine exchanging factor. Phe51 is thought to serve as a hydrophobic grip to be 'pinched off' by the GEF in order to open the switch region, enabling the GEF to dislodge the GDP from its site (online supplemental figure 3).<sup>20</sup>

The recurrent Arg99His variant is predicted to significantly destabilise the region (−1.55 kcal/mol, DynaMut2), with the disruption of one hydrogen-bond stabilising the GDP binding domain (via Asp26, online supplemental figure 2).<sup>12</sup>

Pro131 is not located in an established interacting region of ARF1 and is not in direct contact with GDP.

### Functional assay

The following variants (p.Tyr35His, p.Thr48Ile, p.Phe51Leu, p.Arg99His, p.Lys127Glu, accounting for 11 known individuals) were evaluated by the functional pulldown assay all caused a significant decrease in ARF1 activity (figure 2,  $p < 0.05$ ).

### DISCUSSION

PVNH has been associated with X linked dominant, autosomal recessive and autosomal dominant syndromes.<sup>21–25</sup>

The phenotypic spectrum of ARF1-related disorder includes ID, microcephaly, PVNH and seizures associated with impaired neuronal migration.

ARF1 is a small GTPase which regulates vesicle trafficking and plays a role in cell adhesion molecule turnover.<sup>2,26</sup> Furthermore, ARF1 is implicated in mitochondrial trafficking of endoplasmic reticulum proteins, as well as mitochondrial cholesterol trafficking and fatty acid uptake into the mitochondria.<sup>27</sup> ARF1 acts as a molecular switch by alternating between GDP-bound (inactive) and GTP-bound (active) conformations. This activation is performed at the membrane via GDP/GTP exchange by brefeldin A-inhibited guanine nucleotide exchange factor 2 (BIG2, encoded by *ARFGEF2*). ARF1<sup>GTP</sup> then can initiate vesicle formation through recruitment of various effectors to the membrane including coat proteins and coat protein adaptors.<sup>28</sup> Inhibition of ARF1 has been shown to disrupt neuronal migration, cell-cell adhesion and dendritic Golgi polarisation.<sup>26,29</sup>

It is still unclear whether the pathogenicity of ARF1 variants results from a dominant effect or from ARF1 haploinsufficiency.

Based on gnomAD data, ARF1 is strongly constrained against missense variants.<sup>5,14</sup> GeVIR score, a missense intolerance metric,<sup>30</sup> ranks ARF1 as the 34th most intolerant gene; GeVIR %: ARF1=17.56 (34/19 361), which is consistent with the missense observed/expected upper bound fraction (MOEUF) from gnomAD; MOEUF: ARF1=0.208 (31/19 704).

Up to now, the intolerance of ARF1 for truncating variants has been uncertain. ARF1 loss-of-function observed/expected upper bound fraction (LOEUF) metric=0.402 (3595/19 198) is in favour of intolerance, but with limited statistical significance due to the short coding sequence of ARF1. Moreover, a few heterozygous loss-of-function variants have been identified in control individuals: two males (aged >45 years and >60 years) carrying a 25 nucleotides deletion resulting in frameshift (rs1010202646) in gnomAD V.2.1.1 (non-neuro), and eight individuals carrying multigenic deletions encompassing ARF1 (nsv523935; nsv516409). For additional information, see online supplemental note 1.

Based on clinical data, the pathogenicity mechanism of ARF1 variants remains unsolved. First, as suggested by *ARFGEF2* biallelic loss-of-function mutations<sup>22,31–33</sup> and the clinical overlap of the two syndromes (ID, microcephaly, PVNH, seizures, growth retardation), the defect in neuronal migration is presumed to be caused by reducing the BIG2-ARF1 pathway activity, rather than a gain of function. Furthermore, the two individuals described with truncating variants (one frameshift variant in our cohort and one nonsense variant from Gana *et al*<sup>7</sup>) favour a loss-of-function mechanism through haploinsufficiency, rather than a toxic gain of function. However, this is discordant with the existence of several control individuals with putative loss-of-function variants in ARF1 (rs1010202646; nsv523935; nsv516409). Interestingly, in vitro and in vivo functional assays on ARF1 mutants have shown dominant negative effects. For example, ARF1<sup>T31N</sup>, a constitutively inactive mutant, has been reported to act as dominant negative when overexpressed.<sup>26</sup> The functional assay of Arf1<sup>Y35H</sup> reduced activation previously reported could not discriminate between a toxic gain of function or a loss of function<sup>5</sup> (see online supplemental note 2). Still, to further delineate the exact pathogenicity mechanism, future studies with additional patients will be needed.

The recurrence of the chr1(GRCh38):g.228097627G>A p.(Arg99His) de novo transition in five individuals suggests a highly mutable position, consistent with the CpG nucleotide context (see online supplemental figure 4).

We compared the ability of six in silico prediction tools to discriminate pathogenic missense from benign missense variants. Since MISTIC<sup>34</sup> showed the best performance (online supplemental figure 1), we recommend its use to apply the prediction criteria (PP3 for variants with MISTIC scores >0.90) during the interpretation of future variants in ARF1.

Clinical findings confirm the phenotypic spectrum of a neuronal migration disorder, with severe ID, microcephaly and seizures. Unexpectedly, PVNH appeared to be inconsistent (30%), and seizures were poorly correlated with the presence of PVNH, or any other brain malformation. Seizures types were not consistent either: generalised tonic-clonic epilepsy was present in only one individual (#13). bMRI frequently showed abnormalities related to neuronal migration disorders (microcephaly, corpus callosum hypoplasia, polymicrogyria and PVNH), and occasional small cerebellum, which is uncommon in PVNH. Facial characteristics revealed some more common features, like microretrognathia, but were not universal, even between subjects with the same variant. Visual or hearing defects were frequent.

No major correlation between genotype and phenotype was found. Although of the four verbal individuals (#4, #5, #6, #15), three had alterations of residue Thr48 or Phe51, located in a conserved conformational switch domain.<sup>28</sup> This could suggest an association between alterations of this switch-1 region (residues Gly40 to Phe51) and a milder cognitive phenotype, compared with the other alterations.

Except for the Pro131 residue, all missense variants were located on patently important residues for ARF1 function. We report two different likely pathogenic missense variants on Pro131: one replacing the hydrophobic proline with a positively charged arginine (Pro131Arg), and the other replacing it with another hydrophobic residue (Pro131Leu). This last hydrophobic to hydrophobic change could suggest a proline-specific role of Pro131 in ARF1 function. To our knowledge, Pro131 does not interact with other ARF1 partner. However, proline residues are known to rigidify the peptidic backbone. Pro131 connects the GDP binding loop to the rest of the C-terminal chain. Notably, the precise position and orientation of Asp129 and Lys127 are likely to be crucial for GDP binding. It is possible that Pro131 exerts a favourable constraint to the backbone of this loop, and helps the favourable positioning of GDP binding residues.

Cutaneous and hepatic manifestations among several individuals are rare and still not significant. However, this could suggest some more systemic roles for ARF1, beyond its implication in cortical neurons development. More patients need to be described to investigate this hypothesis.

Interestingly, *C9orf72*, a gene implicated in neuronal degeneration, has recently been reported to act as an effector of ARF1.<sup>35</sup> While none of the subjects in this series had evidence of neurodegeneration, the large number of young subjects makes this an important feature to evaluate in the future, as the natural history of this entity becomes better known.

In summary, we confirm the role of *ARF1* as an autosomal dominant ID gene associated with neuronal migration defects. The phenotypic spectrum is characterised by ID, microcephaly, seizures and PVNH.

#### Author affiliations

<sup>1</sup>Department of Medical Genetics, Groupe Hospitalo-Universitaire Pitié-Salpêtrière, AP-HP, Sorbonne Université, Paris, France

<sup>2</sup>Division of Human Genetics, Cincinnati Children's Hospital Medical Center, Cincinnati, Ohio, USA

<sup>3</sup>Sackler Faculty of Medicine, Tel Aviv University, Tel Aviv, Israel

<sup>4</sup>Service de Génétique Médicale, Centre Hospitalier Universitaire de Bordeaux, Bordeaux, France

<sup>5</sup>Maladies Rares : Génétique et Métabolisme (MRGM), U1211, INSERM, Bordeaux, France

<sup>6</sup>Pediatric and Prenatal Imaging Department, Centre Hospitalier Universitaire de Bordeaux Groupe hospitalier Pellegrin, Bordeaux, France

<sup>7</sup>Département de génétique médicale, CHU Reims, Reims, France

<sup>8</sup>Department of Translational Genomic, Center for Genomic Medicine, King Faisal Specialist Hospital & Research Center, Riyadh, Saudi Arabia

<sup>9</sup>Division of Pediatric Neurology, Department of Pediatrics, Prince Sultan Military and Medical City, Riyadh, Saudi Arabia

<sup>10</sup>PreventionGenetics LLC, Marshfield, Wisconsin, USA

<sup>11</sup>Division of Medical Genetics, Royal University Hospital, Saskatoon, Saskatchewan, Canada

<sup>12</sup>UAB Epilepsy Center, The University of Alabama at Birmingham Hospital, Birmingham, Alabama, USA

<sup>13</sup>Greg Cooper's Laboratory, HudsonAlpha Institute for Biotechnology, Huntsville, Alabama, USA

<sup>14</sup>Gillette Children's Specialty Healthcare, Ann and Robert H Lurie Children's Hospital of Chicago, Chicago, Illinois, USA

<sup>15</sup>Institute of Human Genetics, Technische Universität München, München, Germany

<sup>16</sup>Institute of Neurogenetics, Helmholtz Zentrum München Deutsches Forschungszentrum für Umwelt und Gesundheit, Neuherberg, Germany

<sup>17</sup>Department of Pediatrics, University Hospital Munich, München, Germany

<sup>18</sup>Rady Children's Institute for Genomic Medicine, San Diego, California, USA

<sup>19</sup>Department of Neurology, Medizinische Universität Wien, Wien, Austria

<sup>20</sup>Rady Children's Hospital-San Diego, University of California, San Diego, California, USA

<sup>21</sup>Department of Neuroscience, Rady Children's Institute for Genomic Medicine, San Diego, California, USA

<sup>22</sup>Division of Neurology, Rady Children's Hospital San Diego, San Diego, California, USA

<sup>23</sup>Laboratorio di Genetica Medica, ASST Papa Giovanni XXIII, Bergamo, Italy

<sup>24</sup>Pediatric Department, ASST Papa Giovanni XXIII, Bergamo, Italy

<sup>25</sup>École d'ingénieurs biotechnologies Paris - SupBiotech, Sup'Biotech, Paris, France

<sup>26</sup>CM, INSERM, Paris, France

<sup>27</sup>Department of Neurology, University of California San Francisco Division of Hospital Medicine, San Francisco, California, USA

<sup>28</sup>Department of Medical Genetics, University of Alberta Hospital, Edmonton, Alberta, Canada

<sup>29</sup>ARUP Laboratories, Salt Lake City, Utah, USA

<sup>30</sup>Department of Pathology, University of Utah, Salt Lake City, Utah, USA

<sup>31</sup>Division of Medical Genetics, Department of Pediatrics, University of Utah, Salt Lake City, Utah, USA

<sup>32</sup>Institute of Human Genetics, Klinikum rechts der Isar, School of Medicine, Technical University of Munich, München, Germany

<sup>33</sup>Fachbereich Neuromuskuläre Erkrankungen und klinische Neurophysiologie, Dr. v. Hauner Children's Hospital, Ludwig-Maximilians-Universität, München, Germany

<sup>34</sup>Division of Pediatrics, University of Alberta, Edmonton, Alberta, Canada

<sup>35</sup>Departments of Pediatrics and Medicine, Columbia University, New York City, New York, USA

<sup>36</sup>Divisions of Neonatology, Genetics and Genomic Medicine, Nationwide Children's Hospital, Columbus, Ohio, USA

<sup>37</sup>Department of Pediatrics, The Ohio State University College of Medicine, Columbus, Ohio, USA

<sup>38</sup>Steve and Cindy Rasmussen Institute for Genomic Medicine, Nationwide Children's Hospital, Columbus, Ohio, USA

<sup>39</sup>Divisions of Genetics and Genomic Medicine, Nationwide Children's Hospital, Columbus, Ohio, USA

<sup>40</sup>Sanford Children's Specialty Clinic, Sioux Falls, South Dakota, USA

<sup>41</sup>Department of Pediatrics, University of South Dakota Sanford School of Medicine, Sioux Falls, South Dakota, USA

<sup>42</sup>Department of Medical Genetics, University Medical Center Utrecht, Utrecht, The Netherlands

<sup>43</sup>Laboratories of Genetic Diagnosis, Institut de Génétique Médicale d'Alsace (IGMA), Strasbourg University Hospitals, Strasbourg, France

<sup>44</sup>Génétique médicale, GHRMSA Hôpital Emile Muller, Mulhouse, France

<sup>45</sup>Department of Pediatrics, University of Cincinnati School of Medicine, Cincinnati, Ohio, USA

<sup>46</sup>Service de Pathologie, University Hospital Centre Bordeaux Pellegrin Hospital Group, Bordeaux, France

**Twitter** Jean-Madeleine de Sainte Agathe @JMdeSteAgathe and Ammar Husami @husamia

**Acknowledgements** The authors kindly thank all the individuals and their families involved in this study. The authors also thank Dr Lionel Arnaud (AP-HP, Sorbonne Université, Paris, France) for his infographic guidance. EB is an employee of PreventionGenetics.

**Contributors** Conceptualisation: J-MdSA, AT; data curation: J-MdSA, BP-S, SN, VM, BK, CP, FSA, BT, ErB, KD, MartB, MLT, EmB, MW, IH, JL, MK, KMW, JRF, MI, AC, OC, TT, PB-T, MeIB, KV, F-DM-J, WC, KW, JWO, AH, BPC, BSS, KB, IMdL, BG, MargB, EG, RL, RWS; formal analysis: J-MdSA, TM, BP-S; writing—original draft: J-MdSA; writing—review and editing: J-MdSA, BP-S, BA, PF, JD, FSA, ErB, MLT, MW, JL, MK, ÉLG, KV, WC, KW, JWO, AH, BPC, BSS, RWS, AT; guarantor: J-MdSA.

**Funding** The authors have not declared a specific grant for this research from any funding agency in the public, commercial or not-for-profit sectors.

**Competing interests** None declared.

**Patient consent for publication** Consent obtained from parent(s)/guardian(s).

**Ethics approval** This study was approved by Comité de Protection des Personnes Sud-Ouest et Outre-Mer III, N°: Avis CEBH 2014/09. Participants gave informed consent to participate in the study before taking part.

**Provenance and peer review** Not commissioned; externally peer reviewed.

**Data availability statement** Data are available on reasonable request. The variants described in this work are freely available in ClinVar database (VCV000690284.1, SCV002103097 and SCV002104213 to SCV002104223), and in MobiDetails (<https://mobidetails.iurc.montp.inserm.fr/MD/vars/ARF1>).

**Supplemental material** This content has been supplied by the author(s). It has not been vetted by BMJ Publishing Group Limited (BMJ) and may not have been peer-reviewed. Any opinions or recommendations discussed are solely those of the author(s) and are not endorsed by BMJ. BMJ disclaims all liability and responsibility arising from any reliance placed on the content. Where the content includes any translated material, BMJ does not warrant the accuracy and reliability of the translations (including but not limited to local regulations, clinical guidelines, terminology, drug names and drug dosages), and is not responsible for any error and/or omissions arising from translation and adaptation or otherwise.

**Open access** This is an open access article distributed in accordance with the Creative Commons Attribution Non Commercial (CC BY-NC 4.0) license, which permits others to distribute, remix, adapt, build upon this work non-commercially, and license their derivative works on different terms, provided the original work is properly cited, appropriate credit is given, any changes made indicated, and the use is non-commercial. See: <http://creativecommons.org/licenses/by-nc/4.0/>.

#### ORCID iDs

Jean-Madeleine de Sainte Agathe <http://orcid.org/0000-0002-7753-8226>  
 Ben Pode-Shakked <http://orcid.org/0000-0001-6017-9629>  
 Vincent Michaud <http://orcid.org/0000-0002-5788-392X>  
 Jean Delmas <http://orcid.org/0000-0002-6847-4953>  
 Fowzan S Alkuraya <http://orcid.org/0000-0003-4158-341X>  
 Eric Bend <http://orcid.org/0000-0002-1283-9036>  
 Martina Bebin <http://orcid.org/0000-0003-1264-3428>  
 Michelle L Thompson <http://orcid.org/0000-0001-8134-9017>  
 Emily M Bryant <http://orcid.org/0000-0001-5393-6687>  
 Matias Wagner <http://orcid.org/0000-0002-4454-8823>  
 Martin Krenn <http://orcid.org/0000-0003-3026-3082>  
 Maria Iascone <http://orcid.org/0000-0002-4707-212X>  
 Anna Cereda <http://orcid.org/0000-0002-1317-5657>  
 Eric LeGuern <http://orcid.org/0000-0003-0013-9646>  
 Melanie Brugger <http://orcid.org/0000-0002-6920-8550>  
 Wendy Chung <http://orcid.org/0000-0003-3438-5685>  
 Kathryn N Weaver <http://orcid.org/0000-0002-3991-135X>  
 Ammar Husami <http://orcid.org/0000-0002-4287-2857>  
 Aurélien Trimouille <http://orcid.org/0000-0002-3457-5684>

#### REFERENCES

- Guerrini R, Dobyns WB. Malformations of cortical development: clinical features and genetic causes. *Lancet Neurol* 2014;13:710–26.
- Lian G, Sheen VL. Cytoskeletal proteins in cortical development and disease: actin associated proteins in periventricular heterotopia. *Front Cell Neurosci* 2015;9:99.
- Liu Y, Kahn RA, Prestegard JH. Structure and membrane interaction of myristoylated ARF1. *Structure* 2009;17:79–87.
- Beck R, Prinz S, Diestelkötter-Bachert P, et al. Coatmer and dimeric ADP ribosylation factor 1 promote distinct steps in membrane scission. *J Cell Biol* 2011;194:765–77.
- Ge X, Gong H, Dumas K, et al. Missense-depleted regions in population exomes implicate ras superfamily nucleotide-binding protein alteration in patients with brain malformation. *Npj Genomic Med* 2016;1.
- Monies D, Abouelhoda M, Assoum M, et al. Lessons learned from large-scale, first-tier clinical exome sequencing in a highly consanguineous population. *Am J Hum Genet* 2019;105:879.
- Gana S, Casella A, Cocioglio S, et al. ARF1 haploinsufficiency causes periventricular nodular heterotopia with variable clinical expressivity. *J Med Genet* 2022;59:781–4.
- Sobreira N, Schiettecatte F, Valle D, et al. GeneMatcher: a matching tool for connecting investigators with an interest in the same gene. *Human Mutation* 2015;36:928–30.
- Richards S, Aziz N, Bale S, et al. Standards and guidelines for the interpretation of sequence variants: a joint consensus recommendation of the American college of medical genetics and genomics and the association for molecular pathology. *Genet Med* 2015;17:405–24.
- Wiel L, Baakman C, Gilissen D, et al. MetaDome: pathogenicity analysis of genetic variants through aggregation of homologous human protein domains. *Hum Mutat* 2019;40:1030–8.
- Gueix N, Peitsch MC. SWISS-MODEL and the SWISS-pdbviewer: an environment for comparative protein modeling. *Electrophoresis* 1997;18:2714–23.
- Rodrigues CHM, Pires DEV, Ascher DB. DynaMut2: assessing changes in stability and flexibility upon single and multiple point missense mutations. *Protein Sci* 2021;30:60–9.
- Sehnal D, Bittrich S, Deshpande M, et al. Mol\* viewer: modern web APP for 3D visualization and analysis of large biomolecular structures. *Nucleic Acids Res* 2021;49:W431–7.
- Karczewski KJ, Francioli LC, Tiao G, et al. The mutational constraint spectrum quantified from variation in 141,456 humans. *Nature* 2020;581:434–43.
- Halldorsson BV, Eggertsson HP, Moore KHS, et al. The sequences of 150,119 genomes in the UK biobank. *Nature* 2022;607:732–40.
- Nagy E, Maquat LE. A rule for termination-codon position within intron-containing genes: when nonsense affects RNA abundance. *Trends Biochem Sci* 1998;23:198–9.
- Jaganathan K, Kyriazopoulou Panagiotopoulou S, McRae JF, et al. Predicting splicing from primary sequence with deep learning. *Cell* 2019;176:535–48.
- Zhou F, Dong C, Davis JE, et al. The mechanism and function of mitogen-activated protein kinase activation by ARF1. *Cell Signal* 2015;27:2035–44.
- Liu S, Cerione RA, Clardy J. Structural basis for the guanine nucleotide-binding activity of tissue transglutaminase and its regulation of transamidation activity. *Proc Natl Acad Sci USA* 2002;99:2743–7.
- Renault L, Guibert B, Cherfils J. Structural snapshots of the mechanism and inhibition of a guanine nucleotide exchange factor. *Nature* 2003;426:525–30.
- Parrini E, Ramazzotti A, Dobyns WB, et al. Periventricular heterotopia: phenotypic heterogeneity and correlation with filamin A mutations. *Brain* 2006;129:1892–906.
- Sheen VL, Ganesh VS, Topcu M, et al. Mutations in ARFGEF2 implicate vesicle trafficking in neural progenitor proliferation and migration in the human cerebral cortex. *Nat Genet* 2004;36:69–76.
- Cappello S, Gray MJ, Badouel C, et al. Mutations in genes encoding the cadherin receptor-ligand pair DCHS1 and FAT4 disrupt cerebral cortical development. *Nat Genet* 2013;45:1300–8.
- Broix L, Jagline H, Ivanova E, et al. Mutations in the HECT domain of NEDD4L lead to Akt-mTOR pathway deregulation and cause periventricular nodular heterotopia. *Nat Genet* 2016;48:1349–58.
- Conti V, Carabalona A, Palesi-Pocachard E, et al. Periventricular heterotopia in 6q terminal deletion syndrome: role of the c6orf70 gene. *Brain* 2013;136:3378–94.
- Zhang J, Neal J, Lian G, et al. Filamin A regulates neuronal migration through brefeldin a-inhibited guanine exchange factor 2-dependent ARF1 activation. *J Neurosci* 2013;33:15735–46.
- Andersen J-P, Zhang J, Sun H, et al. Aster-B coordinates with ARF1 to regulate mitochondrial cholesterol transport. *Mol Metab* 2020;42:101055.
- Sztul E, Chen P-W, Casanova JE, et al. ARF GTPases and their GEFs and gaps: concepts and challenges. *MBoC* 2019;30:1249–71.
- Hong E-H, Kim J-Y, Kim J-H, et al. BIG2-ARF1-rhoa-mdia1 signaling regulates dendritic Golgi polarization in hippocampal neurons. *Mol Neurobiol* 2018;55:7701–16.
- Abramovs N, Brass A, Tassabehji M. GeVIR is a continuous gene-level metric that uses variant distribution patterns to prioritize disease candidate genes. *Nat Genet* 2020;52:35–9.
- de Wit MCY, de Coo IFM, Halley DJJ, et al. Movement disorder and neuronal migration disorder due to ARFGEF2 mutation. *Neurogenetics* 2009;10:333–6.
- Bardón-Cancho EJ, Muñoz-Jiménez L, Vázquez-López M, et al. Periventricular nodular heterotopia and dystonia due to an ARFGEF2 mutation. *Pediatr Neurol* 2014;51:461–4.
- Yilmaz S, Gokben S, Serdaroglu G, et al. The expanding phenotypic spectrum of ARFGEF2 gene mutation: cardiomyopathy and movement disorder. *Brain Dev* 2016;38:124–7.
- Chennen K, Weber T, Lornage X, et al. MISTIC: a prediction tool to reveal disease-relevant deleterious missense variants. *PLOS ONE* 2020;15:e0236962.
- Su M-Y, Fromm SA, Zoncu R, et al. Structure of the C9orf72 ARF gap complex that is haploinsufficient in ALS and FTD. *Nature* 2020;585:251–5.
- Morris KL, Buffalo CZ, Stürzel CM, et al. HIV-1 nefs are cargo-sensitive AP-1 trimerization switches in tetherin downregulation. *Cell* 2018;174:659–71.



Supplemental Data of

## **ARF1-related disorder: phenotypic and molecular spectrum.**

Jean-Madeleine de Sainte Agathe MD (1), Ben Pode-Shakked MD (2), Sophie Naudion MD (3), Vincent Michaud MD (3,4), Benoît Arveiler PharmD, PhD (3,4), Patricia Fergelot MD, PhD (3,4), Jean Delmas MD (5), Boris Keren MD, PhD (1), Céline Poirsier MD (6), Fowzan S Alkuraya MD (7), Brahim Tabarki MD (8), Eric Bend PhD, FACMG (9), Kellie Davis MD, FRCPC, FCCMG (10), E. Martina Bebin MD, MPA (11), Michelle L. Thompson PhD (12), Emily Bryant MS (13), Matias Wagner MD (14), Iris Hannibal MD (15), Jerica Lenberg MS, CGC (16), Martin Krenn MD, PhD (17), Kristen Wigby MD, FACMG (18), Jennifer R Friedman MD (19), Maria Iascone PhD (20), Anna Cereda MD (21), TERENCE MIAO (22), Éric Le Guern MD, PhD (1), Emanuela Argilli PhD (23), Elliott H. Sherr MD, PhD (23), Oana Caluseriu MD (24), Timothy Tidwell PhD (25), Pinar Bayrak-Toydemir MD, PhD (26), Caroline Hagedorn PNP, MSN (27), Melanie Brugger MD (28), Katharina Vill MD (29), Francois-Dominique Morneau-Jacob MD (30), Wendy K. Chung MD, PhD (31), Kathryn N. Weaver MD (32), Joshua W. Owens MD (32), Ammar Husami (32), Bimal P. Chaudhari MD, MPH (33), Brandon S. Stone MD (34), Katie Burns MS, CGC (35), Rachel Li MD, MMS (36), Iris M de Lange (37), Margaux Biehler MD (38), Emmanuelle Ginglinger MD (39), Bénédicte Gérard MD (38), Rolf W Stottmann PhD (40), Aurélien Trimouille MD, PhD (4,41)

## **Affiliations**

(1) Département de génétique médicale, Groupe Hospitalo-Universitaire Pitié-Salpêtrière, AP-HP.Sorbonne Université, Paris, France

(2) Division of Human Genetics, Cincinnati Children's Hospital Medical Center, Cincinnati, Ohio, USA; Sackler Faculty of Medicine, Tel-Aviv University, Tel-Aviv, Israel

(3) Service de Génétique Médicale CHU de Bordeaux, F-33000, Bordeaux, France

(4) Univ. Bordeaux, INSERM, Maladies Rares : Génétique et Métabolisme (MRGM), U1211, F-33000 Bordeaux, France

(5) Pediatric and Prenatal Imaging Department, CHU de Bordeaux, France

(6) Département de Génétique, CHU de Reims, Reims, France

(7) Department of Translational Genomic, Center for Genomic Medicine, King Faisal Specialist Hospital and Research Center, Riyadh, Saudi Arabia

(8) Division of Pediatric Neurology, Department of Pediatrics, Prince Sultan Military Medical City, Riyadh, Saudi Arabia

- (9) PreventionGenetics, Marshfield, WI, USA
- (10) Division of Medical Genetics, Royal University Hospital, Saskatoon, Canada
- (11) University of Alabama at Birmingham, Birmingham, AL, USA
- (12) HudsonAlpha Institute for Biotechnology, Huntsville, AL, USA
- (13) Ann & Robert H Lurie Children's Hospital of Chicago; Gillette Children's Specialty Healthcare
- (14) Institute of Human Genetics, Technical University Munich, School of Medicine, Munich, Germany; Institute of Neurogenomics, Helmholtz Zentrum München, Neuherberg, Germany
- (15) Department of Pediatrics, University Hospital München, Munich, Germany
- (16) Rady Children's Institute for Genomic Medicine, San Diego, California, USA
- (17) Department of Neurology, Medical University of Vienna, Austria
- (18) University of California, San Diego, Rady Children's Hospital-San Diego, San Diego, California, USA
- (19) Department of Neuroscience at the University of California, San Diego, San Diego, California; Division of Neurology, Rady Children's Hospital San Diego, San Diego, California
- (20) Laboratorio di Genetica Medica, ASST Papa Giovanni XXIII, Bergamo, Italy
- (21) Department of Pediatrics, ASST Papa Giovanni XXIII, Bergamo, Italy
- (22) Sup'Biotech, Paris, France
- (23) Departments of Neurology and Pediatrics Institute of Human Genetics and Weill Institute for Neurosciences University of California, San Francisco, San Francisco, California
- (23) Departments of Neurology and Pediatrics Institute of Human Genetics and Weill Institute for Neurosciences University of California, San Francisco, San Francisco, California
- (24) Department of Medical Genetics, University of Alberta, Edmonton, AB, Canada
- (25) ARUP Laboratories, Salt Lake City, UT 84108, USA
- (26) Department of Pathology, University of Utah, Salt Lake City, UT, USA; ARUP Laboratories, Salt Lake City, UT 84108, USA
- (27) Division of Medical Genetics, Department of Pediatrics, University of Utah, Salt Lake City, UT, USA

(28) Institute of Human Genetics, Klinikum rechts der Isar, School of Medicine, Technical University of Munich, Munich, Germany

(29) Fachbereich Neuromuskuläre Erkrankungen und klinische Neurophysiologie, Dr. von Haunersches Kinderspital, Munchen, Germany

(30) Division of Pediatrics, University of Alberta, Edmonton, Alberta, Canada

(31) Departments of Pediatrics and Medicine, Columbia University New York NY USA

(32) Division of Human Genetics, Cincinnati Children's Hospital Medical Center, Cincinnati, Ohio, USA

(33) Divisions of Neonatology, Genetics and Genomic Medicine, Nationwide Children's Hospital, Columbus, OH USA; Steve and Cindy Rasmussen Institute for Genomic Medicine, Nationwide Children's Hospital, Columbus, OH, USA; Department of Pediatrics, The Ohio State University College of Medicine, Columbus, OH, USA

(34) Division of Genetics and Genomic Medicine, Nationwide Children's Hospital, Columbus, OH USA; The Ohio State University College of Medicine, Columbus, OH, USA

(35) Sanford Children's Specialty Clinic, Sioux Falls, South Dakota, USA

(36) Department of Pediatrics, Sanford School of Medicine of the University of South Dakota, Sioux Falls, SD, USA

(37) Department of Medical Genetics, University Medical Center Utrecht, Utrecht University, Utrecht, The Netherlands.

(38) Laboratories of Genetic Diagnosis, Institut de Génétique Médicale d'Alsace (IGMA), Strasbourg University Hospitals, Strasbourg, France

(39) Génétique médicale, Hôpital Emile Muller, Mulhouse, France

(40) Division of Human Genetics, Cincinnati Children's Hospital Medical Center, Cincinnati, Ohio, USA; Department of Pediatrics, University of Cincinnati School of Medicine, Cincinnati, Ohio, USA

(41) Service de Pathologie CHU de Bordeaux, F-33000, Bordeaux, France

\* current address: Steve and Cindy Rasmussen Institute for Genomic Medicine, Nationwide Children's Hospital, Columbus, OH, USA; Department of Pediatrics, The Ohio State University College of Medicine, Columbus, OH, USA

#### Corresponding author:

Jean-Madeleine de Sainte Agathe MD, jean-madeleine.desainteagathe@aphp.fr



## Supplementary note 1:

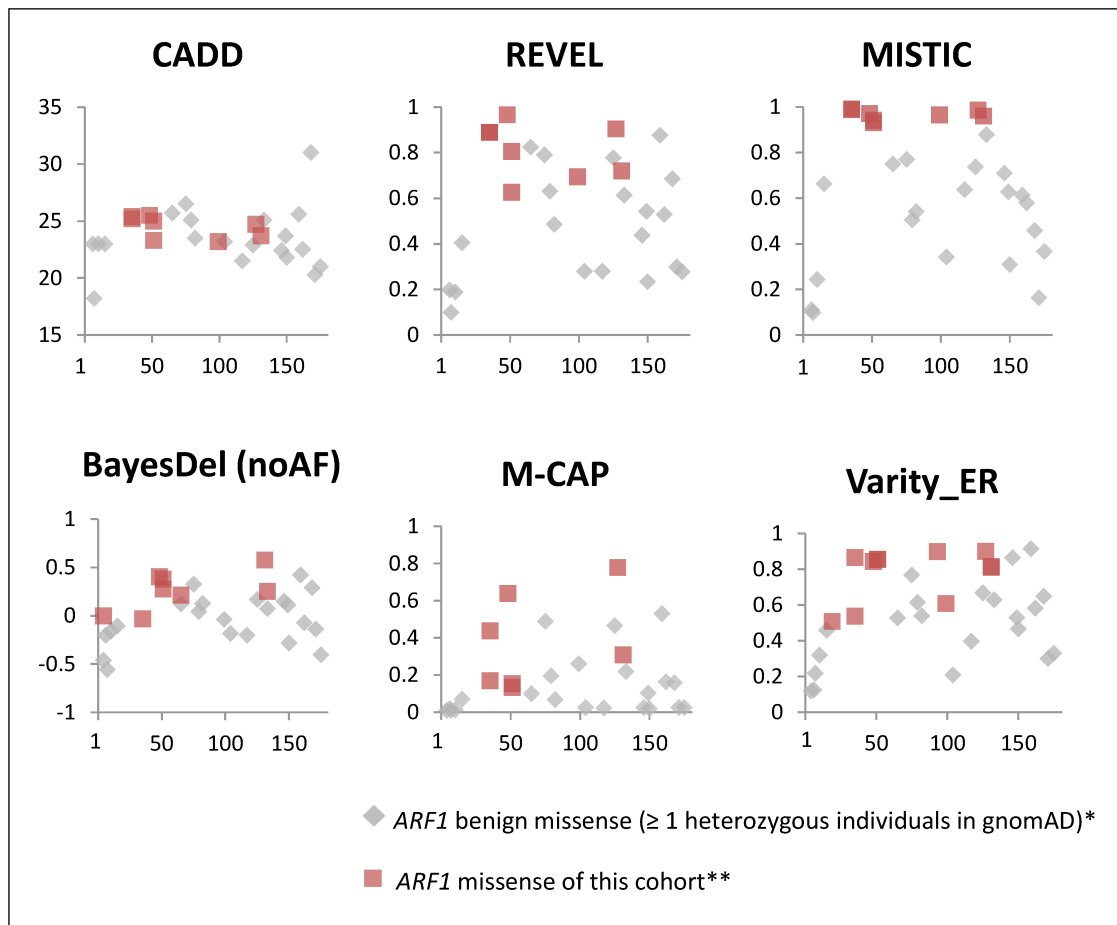
During the compilation of *ARF1* putative loss-of-function variant, we excluded four gnomAD individuals with presumed loss-of-function variants. Indeed, two individuals in gnomADv2.1.1 (rs755638275, available at [https://gnomad.broadinstitute.org/variant/1-228285417-G-GACCTCCCCAACGCCATGAATGCGGCCGAGATCACAGACAAGCTGGGGCTGCAC?dataset=gnomad\\_r2\\_1](https://gnomad.broadinstitute.org/variant/1-228285417-G-GACCTCCCCAACGCCATGAATGCGGCCGAGATCACAGACAAGCTGGGGCTGCAC?dataset=gnomad_r2_1)); and at [https://gnomad.broadinstitute.org/variant/1-228285417-G-GACC?dataset=gnomad\\_r2\\_1](https://gnomad.broadinstitute.org/variant/1-228285417-G-GACC?dataset=gnomad_r2_1)) and two individuals in gnomAD v3.1.1 (79 nucleotides deletion, c.148+2\_149del, available at [https://gnomad.broadinstitute.org/variant/1-228097260-TAGGTGAGGTGGGGCCAGCAGGGAGTGGGCTGGGCTGGGCTGGGCCAAGGTACAAGGCCTCACCCTGCATCCCGCACCC-T?dataset=gnomad\\_r3](https://gnomad.broadinstitute.org/variant/1-228097260-TAGGTGAGGTGGGGCCAGCAGGGAGTGGGCTGGGCTGGGCTGGGCCAAGGTACAAGGCCTCACCCTGCATCCCGCACCC-T?dataset=gnomad_r3)) were identified with alleles predicted to be splice disruptive but could not be counted as germline loss-of-function variants with enough confidence after examination. We observed the following issues: long alternative alleles matching a processed pseudogene and poor read support. The two variants in gnomADv2.1.1 (rs755638275) had high strand bias (Phred-scaled p-value of Fisher's exact test = 45.347) and a very low QD score (QD < 6), which failed to meet satisfying confidence for germline variants. Alternative alleles were compatible with a processed pseudogene (inserted/deleted nucleotides concordant with exon4/exon5 junction, intronic heterozygous SNV present in the supposedly heterozygous 79pb deletion). This issue has been submitted to gnomAD production team and resulted in the suppression of the read data of the gnomAD v3.1.1 individuals.

## Supplementary note 2:

The *in-vitro* activation of Arf1<sup>Y35H</sup> in transfected cells previously reported was weaker compared to Arf1<sup>WT</sup> transfected cells but stronger compared to basal activation, which is compatible with the Arf1 overexpression in transfected cells compared to non-transfected cells.<sup>1</sup>

## Supp. Fig. 1

- A) Missense deleteriousness predictions from CADD (GRCh37-v1.6), REVEL, MISTIC, BayesDel (noAF), M-CAP and Varsity\_ER of benign *ARF1* missense variants, and pathogenic variants of this cohort (eight substitutions, seven distinct missense variations, red).<sup>2-7</sup> Vertical axis: deleterious prediction scores; horizontal axis: *ARF1* residues.

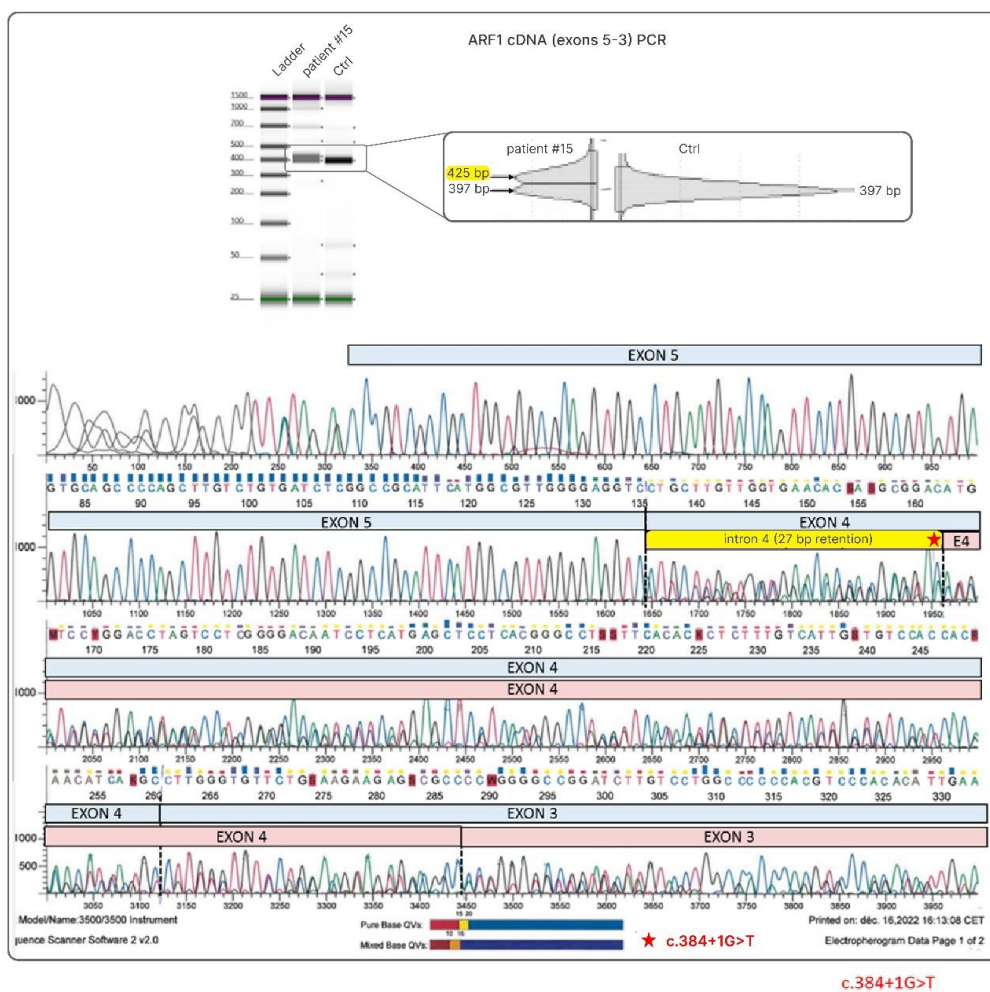
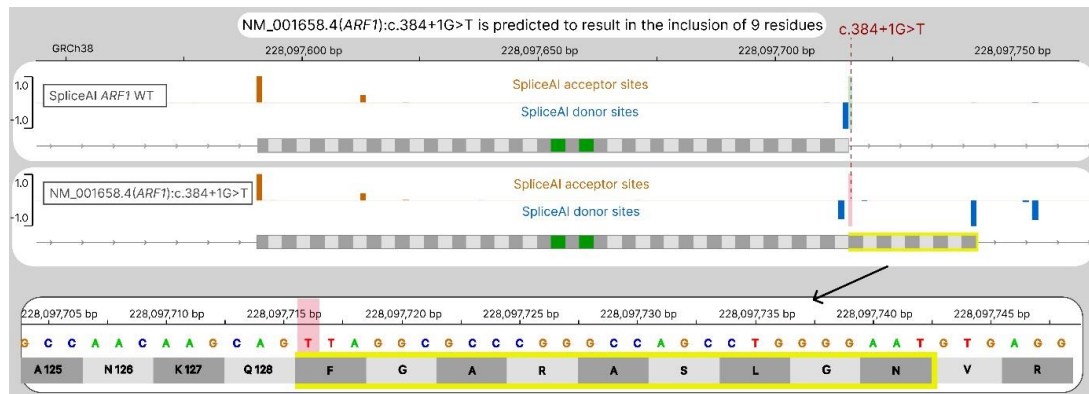


\* One missense variant in gnomADv3.1 (1-228097853-A-C (GRCh38); p.(Asp129Ala), available at: [https://gnomad.broadinstitute.org/variant/1-228097853-A-C?dataset=gnomad\\_r3](https://gnomad.broadinstitute.org/variant/1-228097853-A-C?dataset=gnomad_r3)) has been excluded from this analysis because of highly suspicious quality metrics (QD=1.136) and poor read support for germline heterozygous substitution (allelic fraction of 29% based on 5/17 reads and 3/5 having a base quality <7). This issue has been reported to gnomAD Production Team.

\*\* The better discrimination superiority of MISTIC was not biased by the presence of three missense variants in HGMD<sup>8</sup> or ClinVar<sup>9</sup> (p.Y35H, p.R99H and p.K127E), since the positive training sets used for MISTIC did not include these variants or any other variants of our cohort.

MISTIC discriminates pathogenic from benign variants with better accuracy than CADD, M-CAP, BayesDel, REVEL or Varsity. Potential splicing alteration of the cohort variants were investigated with spliceAI, which predicted no impact.<sup>10</sup>

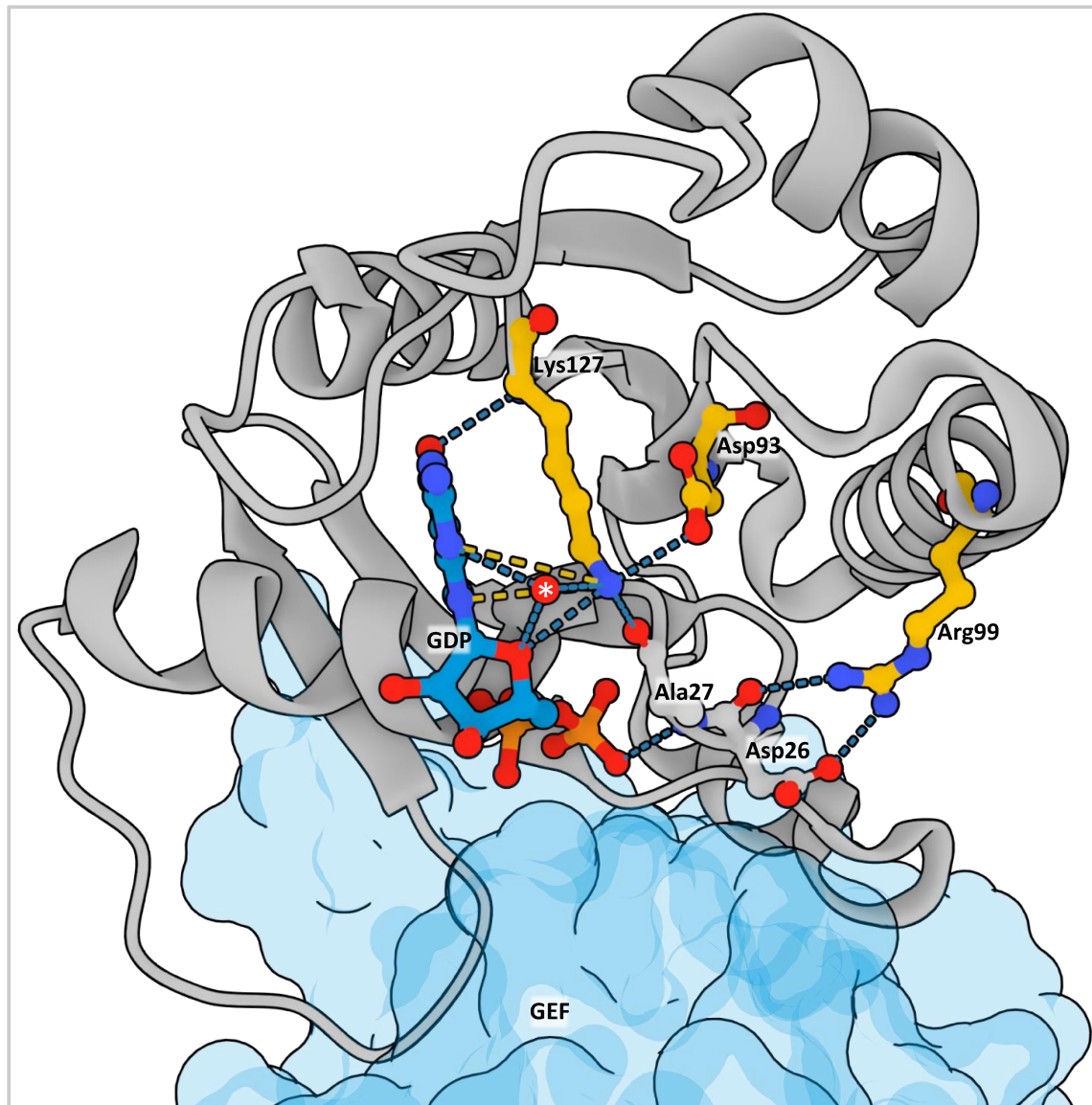
- B) RNA results for NM\_001658.4(*ARF1*):c.384+1G>T. Above panel showing SpliceAI-visual predictions.<sup>11</sup> Above: predictions for the wild-type sequence, middle: predictions for the c.384+1G>T variant, below: close-up of the predicted amino-acid sequence inserted after Gln128. The variant is highlighted in red. Below panel showing ARF1 cDNA PCR and Sanger analysis.



## Supp. Fig. 2

Stabilization of the Lys127 sidechain by Asp93. The second phosphate of GDP is interacting with the Ala26-Asp27 backbone, in close contact with Arg99.

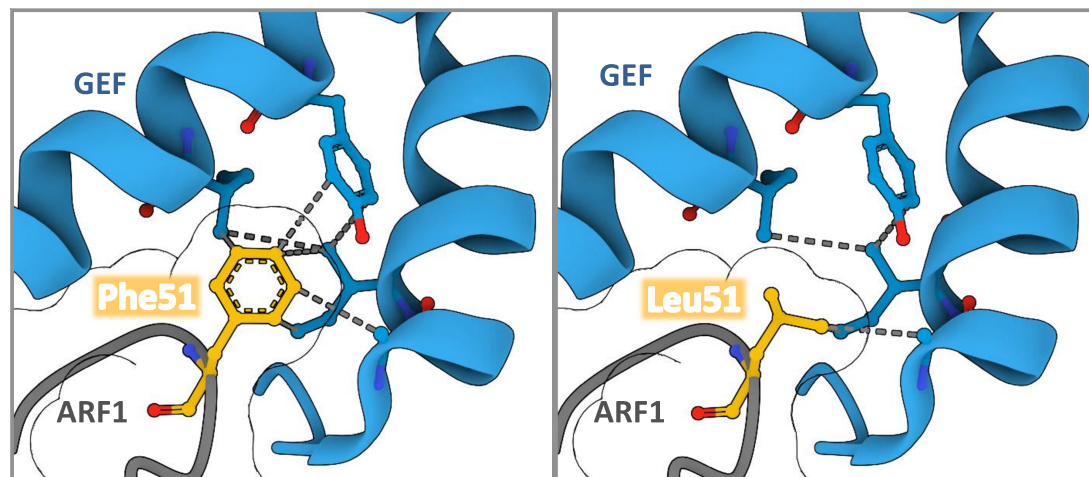




Structure of ARF1 (grey cartoon) in its inactive GDP-bound conformation (1r8s)<sup>12</sup>, with 3 mutated residues in yellow. Dashed blue lines: H-bonds; dashed yellow lines: ionic bonds; the red ball marked by a white asterisk represents H<sub>2</sub>O molecule.

### Sup. Fig. 3

GEF uses Phe51 hydrophobic ring to 'pinch off' ARF1 switch loop. This interaction is required for the GEF to push out the GDP during activation of ARF1. The Phe to Leu missense is likely to alter the strength of this interaction.



In blue and in grey: GEF, ARF1, respectively, according to the structure 1s9d (right) or to the modelled Phe51Leu by Swiss-Model using 1s9d as template (left). Grey dashed lines: hydrophobic interactions.

### Supp. Fig. 4

Molecular hypothesis for recurrence of chr1(GRCh38):g.228097627G>A p.(Arg99His).

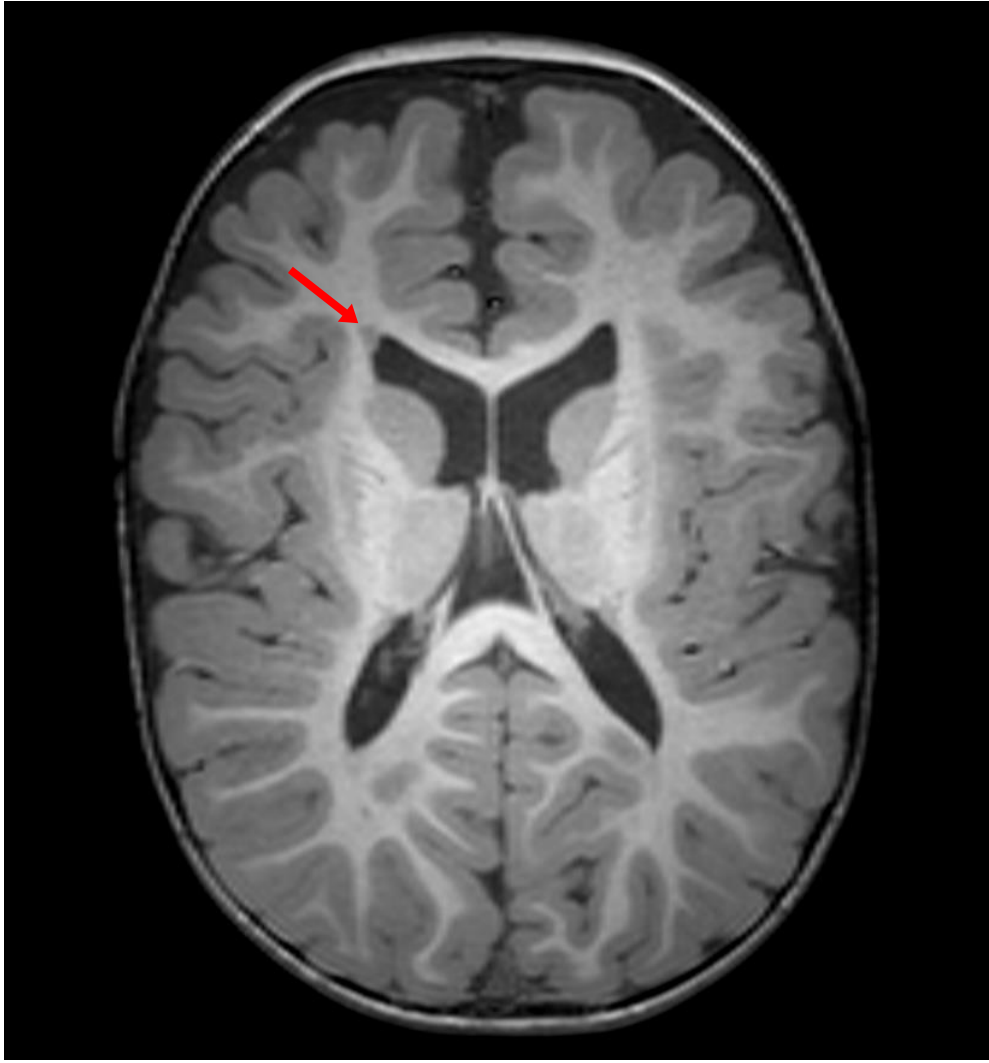


The nucleotidic context of the recurrent substitution is compatible with a spontaneous deamination of a methylated cytosine, known to be in high proportion among de novo substitutions.<sup>13</sup> The methylated cytosine ("m", in red: methyl radical), spontaneously deaminates in thymine (red "T"), followed by mismatch repair. NB: in this figure, only the incorrect mismatch repair causing the missense is shown (strand +, G>A), the correct mismatch repair (strand -, T>C) is not depicted.

## Supp. Fig 5. Brain MRI images

---

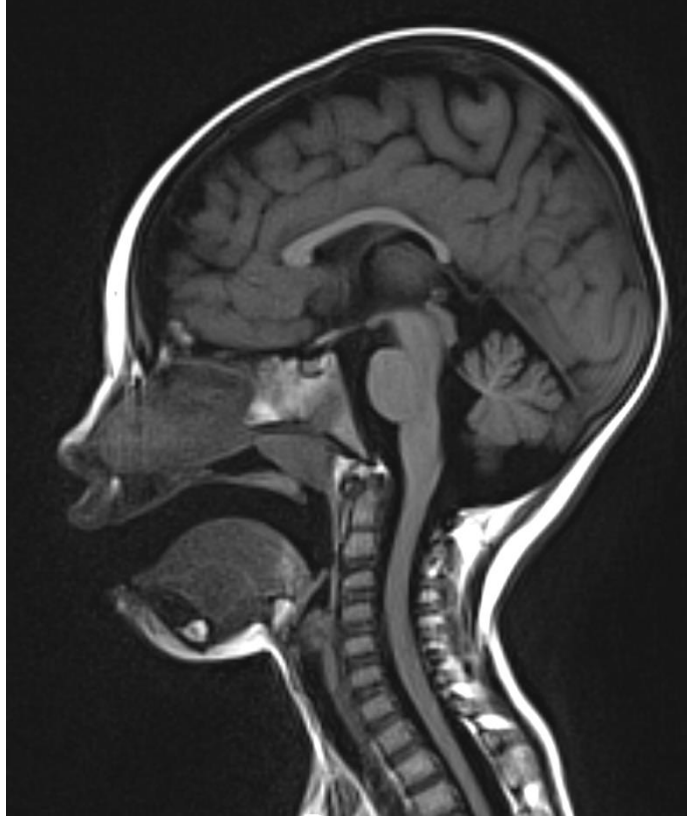
- A) Individual #1, 2 years, axial T1-weighted MRI section showing periventricular nodular heterotopia.



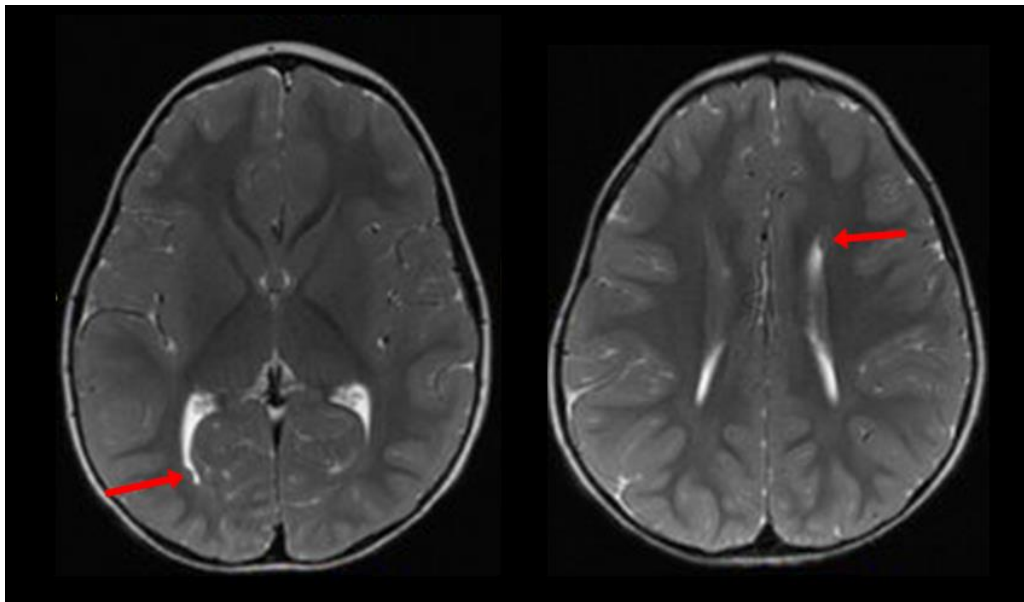
- B) Individual #9, 12 years old. Sagittal T1-weighted section showing relative microcephaly, cerebral atrophy, partial hypoplasia of corpus callosum (especially posterior), and cerebellar vermis hypoplasia. Axial T2-weighted sections showing bilateral enlargement of parietal subarachnoid spaces.



- C) Individual #11, 2 years old. Sagittal T1-weighted section showing thin aspect of the corpus callosum (more pronounced at the splenium), relative microcephaly and cerebellar vermis hypoplasia.



D) Individual #13, age unknown, T2-weighted sections showing PNH (red arrows).



#### Supplemental data references

---

1. Ge X, Gong H, Dumas K, et al. Missense-depleted regions in population exomes implicate ras superfamily nucleotide-binding protein alteration in patients with brain malformation. *Npj Genomic Med.* 2016;1(1):16036. doi:10.1038/npjgenmed.2016.36
2. Rentzsch P, Witten D, Cooper GM, Shendure J, Kircher M. CADD: predicting the deleteriousness of variants throughout the human genome. *Nucleic Acids Res.* 2019;47(D1):D886-D894. doi:10.1093/nar/gky1016
3. Ioannidis NM, Rothstein JH, Pejaver V, et al. REVEL: An Ensemble Method for Predicting the Pathogenicity of Rare Missense Variants. *Am J Hum Genet.* 2016;99(4):877-885. doi:10.1016/j.ajhg.2016.08.016
4. Chennen K, Weber T, Lornage X, et al. MISTIC: A prediction tool to reveal disease-relevant deleterious missense variants. Andrade-Navarro MA, ed. *PLOS ONE.* 2020;15(7):e0236962. doi:10.1371/journal.pone.0236962
5. Feng BJ. PERCH: A Unified Framework for Disease Gene Prioritization: HUMAN MUTATION. *Hum Mutat.* 2017;38(3):243-251. doi:10.1002/humu.23158
6. Jagadeesh KA, Wenger AM, Berger MJ, et al. M-CAP eliminates a majority of variants of uncertain significance in clinical exomes at high sensitivity. *Nat Genet.* 2016;48(12):1581-1586. doi:10.1038/ng.3703
7. Wu Y, Liu H, Li R, Sun S, Weile J, Roth FP. Improved pathogenicity prediction for rare human missense variants. *Am J Hum Genet.* 2021;108(10):1891-1906. doi:10.1016/j.ajhg.2021.08.012

8. Stenson PD, Ball EV, Mort M, et al. Human Gene Mutation Database (HGMD<sup>®</sup>): 2003 update: HGMD 2003 UPDATE. *Hum Mutat*. 2003;21(6):577-581. doi:10.1002/humu.10212
9. Landrum MJ, Lee JM, Benson M, et al. ClinVar: improving access to variant interpretations and supporting evidence. *Nucleic Acids Res*. 2018;46(D1):D1062-D1067. doi:10.1093/nar/gkx1153
10. Jaganathan K, Kyriazopoulou Panagiotopoulou S, McRae JF, et al. Predicting Splicing from Primary Sequence with Deep Learning. *Cell*. 2019;176(3):535-548.e24. doi:10.1016/j.cell.2018.12.015
11. de Sainte Agathe JM, Filser M, Isidor B, et al. SpliceAI-visual: a free online tool to improve SpliceAI splicing variant interpretation. *Hum Genomics*. 2023;17(1):7. doi:10.1186/s40246-023-00451-1
12. Renault L, Guibert B, Cherfils J. Structural snapshots of the mechanism and inhibition of a guanine nucleotide exchange factor. *Nature*. 2003;426(6966):525-530. doi:10.1038/nature02197
13. UK10K Consortium, Rahbari R, Wuster A, et al. Timing, rates and spectra of human germline mutation. *Nat Genet*. 2016;48(2):126-133. doi:10.1038/ng.3469